Mean-field theory of two-dimensional metallic photonic crystals

G. Guida, D. Maystre, G. Tayeb, and P. Vincent

Laboratoire d'Optique Electromagnétique, Unité Propre de Recherche de l'Enseignement Supérieur A 6079, Faculté des Sciences et Techniques de St-Jérôme, Case 262, Avenue Escadrille Normandie-Niemen, 13397 Marseille Cedex 20, France

Received September 23, 1997; revised manuscript received March 31, 1998

Metallic photonic crystals have gaps starting from the null frequency. They can be used as antenna substrates. Using two computer codes based on rigorous scattering theories, we investigate the properties of nondoped and doped two-dimensional metallic photonic crystals. We show numerically that such a structure can simulate a material that has a plasmon frequency in the microwave domain. Below this frequency the crystal is opaque and acts as a good reflector. These calculations confirm both a conjecture made by specialists in solid-state physics and mathematical considerations developed by specialists in limit analysis. © 1998 Optical Society of America [S0740-3224(98)04307-0]

OCIS code: 250.0250

1. INTRODUCTION

Photonic band structures have attracted increasing interest in recent years. One objective of the studies in this field is to find structures that are able to provide complete control of light propagation.[1–8] Most of the experimental and theoretical studies in the field of photonic crystals are devoted to dielectric photonic crystals. Even though dielectric photonic crystals are able to control propagation of light in the microwave region, most practical applications of the properties of these structures are found in the infrared and visible ranges. Let us recall that their most famous property, the inhibition of spontaneous emission of atoms and molecules, could permit the construction of zero-threshold lasers and single-mode light-emitting diodes. However, the construction of such photonic crystals in the optical range remains a quite difficult challenge.

We are here concerned with another kind of photonic band structure: the metallic photonic crystal. In contrast with the dielectric photonic crystal, which in general has gaps limited to an octave or less (the interested reader can refer to Refs. 3, 5, 7, and 9 for examples of such gaps for doped and nondoped crystals), the metallic photonic crystal can generate gaps extending from zero frequency to a cutoff value. The other vital difference between a metallic photonic crystal and a dielectric one is that the former is intended to work mainly in the microwave region, for instance as an efficient microwave reflector or microwave cavity (the interested reader can refer to Refs. 10–15 for more details), whereas the latter is devoted to the visible and infrared regions, for practical applications mentioned above. The metallic crystals that we are dealing with in this paper are made with a two-dimensional (2D) periodic array of parallel perfectly conducting rods.

Numerical investigations have been carried out with two computer codes. The first code[5] allows us to deal with a superposition of a finite set of 2D grids of infinite extension; the second is intended to solve the scattering problem for a nonperiodic structure made with parallel rods.[16] The second code enables us to investigate the scattering properties of doped or finite-sized photonic crystals or both. Both codes are based on rigorous theories of scattering.

Using these codes, we studied the shape and the limits of the gaps. Special attention was paid to the case of doped crystals, in which peaks of transmission can appear in the gap. We are able to confirm the conjecture of specialists in solid-state physics[17] that a metallic photonic crystal can simulate a homogeneous material, the plasmon frequency of which is located in the microwave domain. Up to this plasmon frequency, the permittivity of the material is negative and the crystal is a good reflector. For greater frequencies the permittivity is positive and the material becomes a classic dielectric medium.

We show that a mathematical formula deduced from the theory of limit analysis provides a good estimate of the permittivity of a homogenized material as a function of frequency.[18,19] It is worth noting that the mean-field limit is equivalent to the low-k limit relative to the k value at the Brillouin zone boundary.

2. THEORY AND NUMERICAL IMPLEMENTATION IN OUTLINE

A. Grating Theory

The first code that we use to investigate the properties of 2D metallic photonic crystals is aimed toward the solution of a general grating problem. It is able to compute with a precision better than 1% in relative value the fields scattered by arbitrary gratings, especially those used for commercial applications (sinusoidal, rectangular, or triangular groove gratings) but also gratings made with rods. This code has been elaborated from a rigorous integral theory, which reduces the grating problem to a system of coupled integral equations. From the concept of scatter-

 © 1998 Optical Society of America

ing matrix, it allows one to deal with a stack of grating profiles or grids, provided that the periods of all the elementary gratings of the stack are identical.[5] The validity of the code has been verified by classic tests (reciprocity, energy balance, convergence of the results when the size of the linear system of equations to be solved is increased, etc.) and above all by numerous comparisons with experimental data. Let us recall that an older version of this code allowed us to predict the phenomenon of total absorption of light by a metallic grating in the visible region,[20] which was verified experimentally.[21]

B. Theory of Scattering by a Finite Set of Parallel Rods

A code that deals with gratings is able to compute the limits of the gaps of a photonic crystal but is quite unable to predict the effects of the limited size of the crystal in any direction or the properties of doped crystals, viz., crystals for which the periodicity has been broken. For this reason we have used a second code, which deals with the problem of scattering by a finite number of arbitrarily shaped parallel cylindrical rods. In outline, the rigorous theory can be decomposed into two steps. First, the scattering matrices of all the rods are calculated separately. Then the scattering matrix of the entire set of rods is deduced from all the elementary scattering matrices by inversion of a complex matrix.[16] As for the grating code, numerous numerical tests, including comparisons with other codes, have been performed, and one can consider that the relative accuracy of our numerical results is better than 1%.

3. NUMERICAL STUDY OF TWO-DIMENSIONAL METALLIC PHOTONIC CRYSTALS WITH THE GRATING MODEL

In this section we represent the metallic photonic crystal by a superposition of N_g infinite grids that have the same period d and are vertically spaced by the same length d (see Fig. 1). The wires have a radius r, and the incident plane wave of wavelength $\lambda = 2\pi c/\omega$ illuminates the grating with incidence angle α, the incident wave vector lying in the xy plane. The x axis contains the centers of the wires of the upper grid. The incident field is TE (or s) polarized, which means that the electric field is parallel to the wires. In practice, the radius r of the rods of the metallic photonic crystal is much smaller than the wavelength λ and the period d. In these conditions the rods are transparent for TM (p) polarization, which explains why TM polarization is not studied what follows. Throughout this paper the period d will be taken equal to 1.

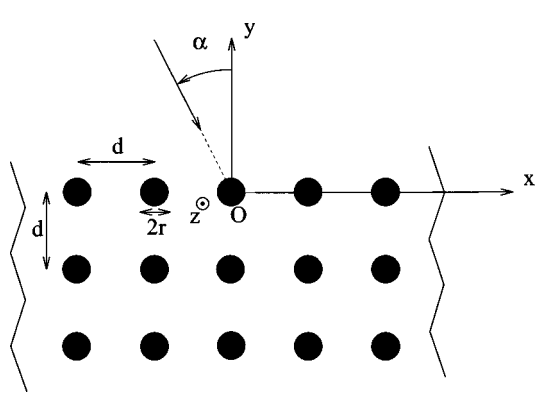

Fig. 1. 2D metallic photonic crystal represented by a grating model with $N_g = 3$. The grids are infinite along the x and z directions.

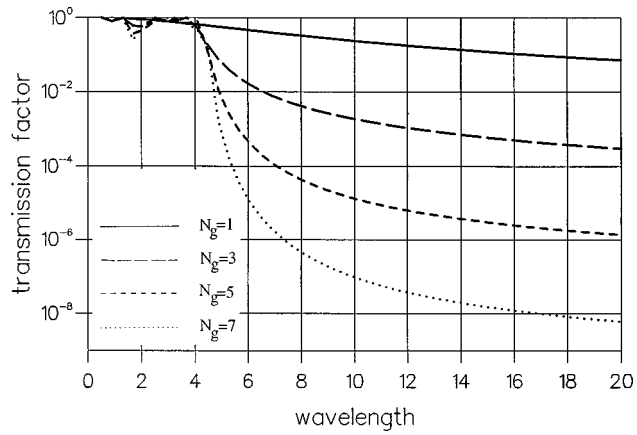

Fig. 2. Transmission factor of a metallic photonic crystal made by perfectly conducting wires of radius $r = 0.01d$ illuminated in normal incidence.

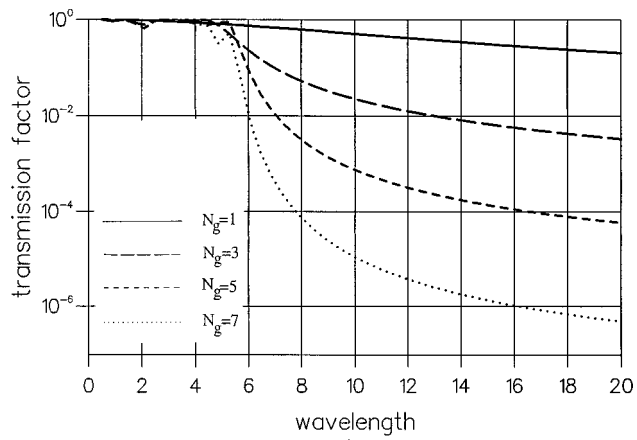

Fig. 3. Same as Fig. 2 but for $r = 0.001d$.

A. Photonic Bandgaps

Figures 2 and 3 show the transmission factor versus the wavelength/period ratio for various values of N_g and for two values of r/d. The main feature of these transmission curves is the existence of a forbidden gap that extends from the cutoff wavelength λ_c to infinity, where λ_c is close to 5 for $r/d = 0.01$ and close to 6 for $r/d = 0.001$. It is worth noting that with very thin wires ($r/d = 0.001$) the transmission factor at $\lambda = 2\lambda_c$ can be smaller than 10^{-3} for $N_g = 5$ and smaller than 10^{-5} for $N_g = 7$.

B. Mean-Field Theory for Metallic Photonic Crystals

Figures 2 and 3 suggest that a metallic photonic crystal could behave as a homogeneous material with properties close to those of a dielectric for $\lambda < \lambda_c$ and close to a finitely conducting metal for $\lambda > \lambda_c$. Specialists in solid-state physics[17,22] have suggested that this homogeneous material could be comparable with a classic metal, but with a plasmon frequency in the microwave region, at

least when the value of the period d (thus of λ_c) lies in this domain. Furthermore, Felbacq,[18] and Felbacq and Bouchitté[19] showed that asymptotically, when d/λ and

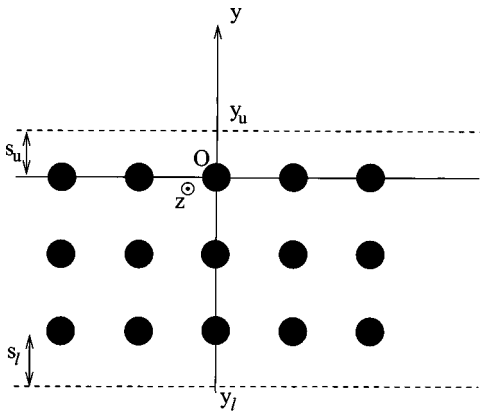

Fig. 4. Layout of the photonic crystal and the equivalent homogeneous layer.

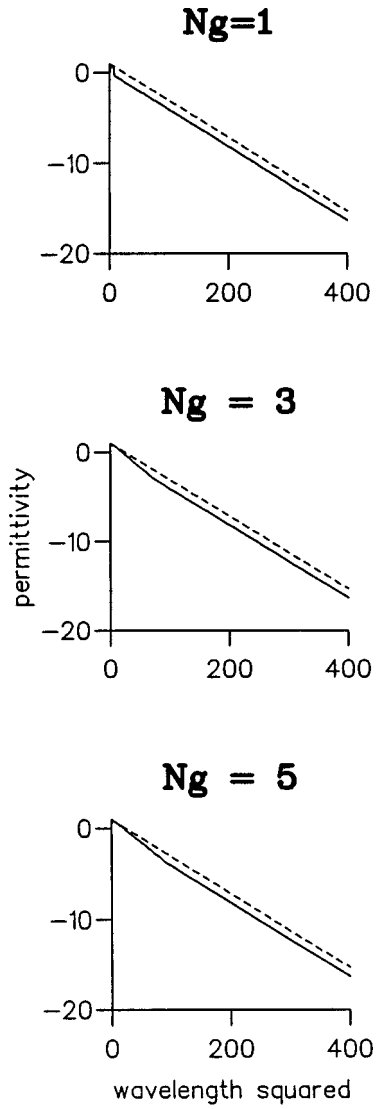

Fig. 5. Permittivity ϵ of the homogeneous material equivalent to a metallic photonic crystal with rods of radius $r = 10^{-2}$ illuminated with normal incidence. Solid curves, numerical result; dashed curves, theoretical result of Eq. (1).

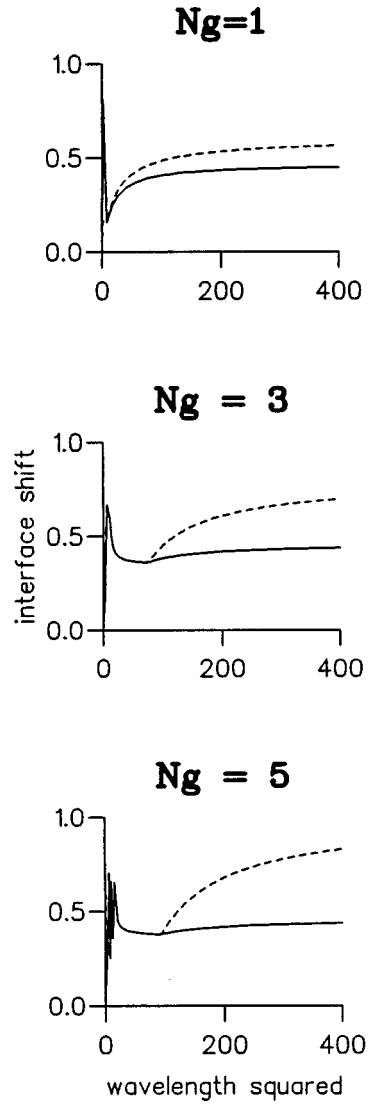

Fig. 6. Same as Fig. 5 but for interface shifts s_u (solid curves) and s_l (dashed curves).

r/λ tend to 0 in a convenient way, the relative permittivity of the homogenized material can be deduced from the crystal parameters by the following formulas:

$$\epsilon_h = 1 - \frac{\omega_p^2}{\omega^2} = 1 - \frac{\lambda^2}{\lambda_p^2}, \tag{1}$$

with

$$\omega_p = \frac{c}{d}\left[\frac{2\pi}{\ln(d/2r)}\right]^{1/2}, \tag{2}$$

$$\lambda_p = \frac{2\pi c}{\omega_p} = d[2\pi \ln(d/2r)]^{1/2}. \tag{3}$$

To check the precision of this formula we computed the reflection and transmission coefficients of a metallic photonic crystal made with N_g grids (Fig. 4). Then we used an iterative technique of minimization to find the real permittivity ϵ and the ordinates y_u and y_l of the upper and lower interfaces of a homogeneous thin film that has the same reflection and transmission coefficients as the crystal. Because ϵ is real (the wires are perfectly con-

ducting, so the material must be lossless), we have to find three parameters, ϵ, y_u, and y_l, from four real parameters (real and imaginary parts of r and t). In fact, the photonic crystal is lossless, and thus r and t must satisfy the energy balance criterion

$$|r|^2 + |t|^2 = 1, \tag{4}$$

which means that the data contain three independent real parameters as well as the result of the optimization. We used an iterative technique for which the initial value of ϵ is given by Eqs. (1) and (2) and the initial values of y_u and y_l are chosen as the actual boundaries of the crystal. The shifts s_u and s_l of the upper and the lower interfaces, respectively, are defined by

$$s_u = y_u, \tag{5}$$

$$s_l = -(N_g - 1)d - y_l. \tag{6}$$

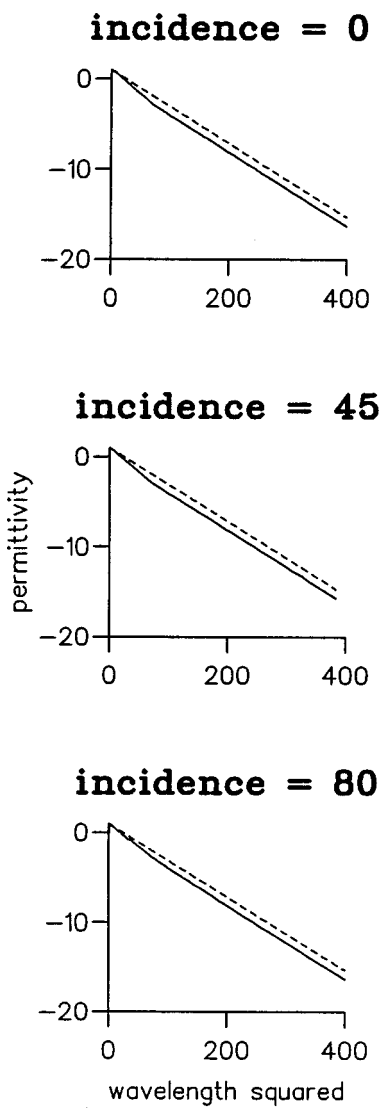

Fig. 7. Permittivity ϵ of the homogeneous material equivalent to a metallic photonic crystal with radius $r = 0.01$ made with $N_g = 3$ grids, for three values of incidence angle α (in degrees). Solid curves, numerical result, dashed curves, theoretical result obtained from Eqs. (1) and (2).

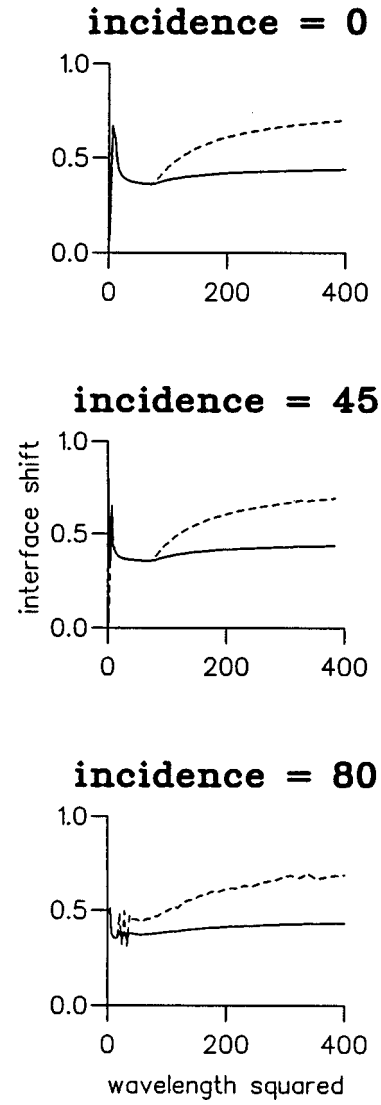

Fig. 8. Same as Fig. 7 but for interfaces s_u (solid curves) and s_l (dashed curves).

Figures 5 and 6 show the permittivity ϵ and the interface shifts of homogeneous material equivalent to a 2D metallic photonic crystal for $N_g = 1,3,5$. The main conclusion that can be drawn from these figures is that the theoretical prediction of ϵ given by Eqs. (1) and (2) is highly accurate; the difference between the numerical and the theoretical values is of the order of unity. It is interesting that above $\lambda \simeq 8$ the difference $\epsilon_h - \epsilon$ remains almost constant; the region $\lambda < 8$ is (for $N_g = 3, 5$) a transition region where $\epsilon - 1$ remains almost linear. It is quite surprising to see that a model in which the metallic photonic crystal is reduced to one grid only ($N_g = 1$) provides a good numerical estimate of the permittivity of the homogenized material obtained for largest values of N_g. Except for the smallest values of λ, the interface shifts s_u and s_l are close to each other ($\sim d/2$). The largest values of s_l when $\lambda > 10$ have a numerical origin: In these conditions the photonic crystal is opaque and the relative precision on the transmission coefficient t decreases as λ is increased. This fact prevents us from making calculations for large values of N_g. Figures 7 and 8 show that a

variation of the incidence α does not result in a big change for the permittivity and the interface shifts.

Figures 9–12 provide a set of curves equivalent to Figs. 5–8 but with $r = 0.001$, the calculation being made with $N_g = 3, 5$ only. The conclusion remains almost the same, except for the linear behavior of $\epsilon - 1$ as a function of λ^2, at least in normal incidence.

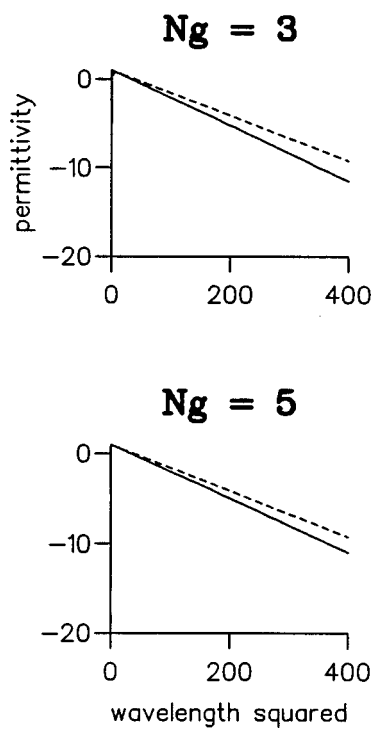

Fig. 9. Same parameters as in Fig. 5 but with $r = 0.001$.

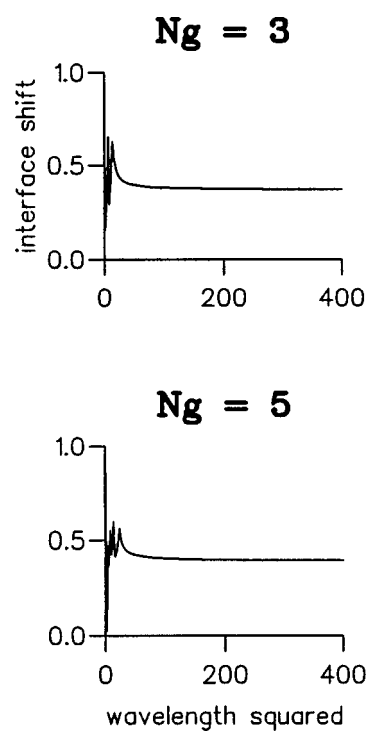

Fig. 10. Same parameters as in Fig. 6 but with $r = 0.001$. The solid and dashed curves are superposable.

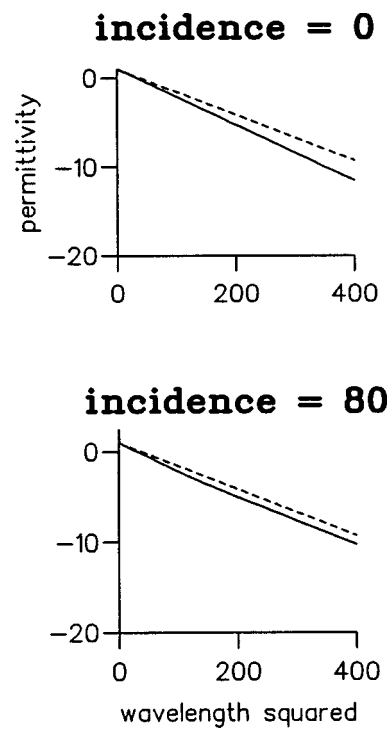

Fig. 11. Same parameters as in Fig. 7 but with $r = 0.001$.

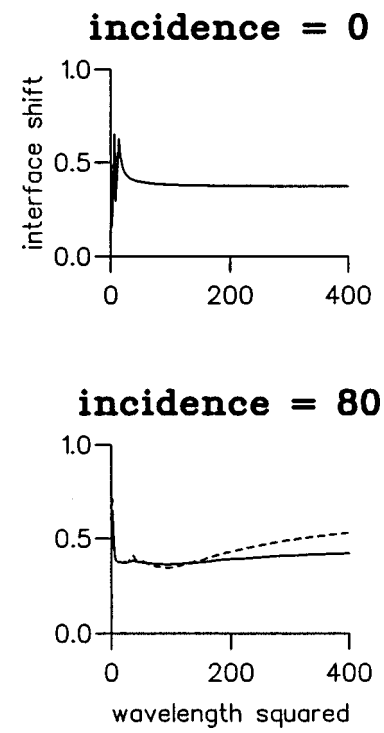

Fig. 12. Same parameters as in Fig. 8 but with $r = 0.001$.

The good agreement of the numerical results with Eqs. (1) and (2) is surprising, at least for the smallest values of λ. Indeed, the theoretical demonstration of these formulas was made under the assumption that λ is much greater than d.

Thus it can be concluded that Eqs. (1) and (2) provide an accurate approximation of the properties of a metallic photonic crystal, provided that the upper and the lower

interfaces of the homogenized material are translated by $d/2$ outside the limits of the crystal. Furthermore, the plasmon wavelength λ_p defined in Eq. (3) gives a useful approximation of the cutoff wavelength λ_c.

4. NUMERICAL STUDY OF TWO-DIMENSIONAL METALLIC PHOTONIC CRYSTALS WITH THE NONPERIODIC MODEL

In this section we perform the study with the help of the second code described briefly in Subsection 2.B above (the interested reader can find more details of the theory in Refs. 9 and 16). Wires still have an infinite length, but the number of wires is finite, and their positions can be arbitrary, which enables us to study the influence of defects in the crystal. The code is also able to easily give the field structure inside the crystal, for instance, by drawing field maps, which is helpful to our understanding of the properties of such crystals. The scheme of the study remains the same as in Section 3, and we keep the same parameters: s polarization and period d equal to 1.

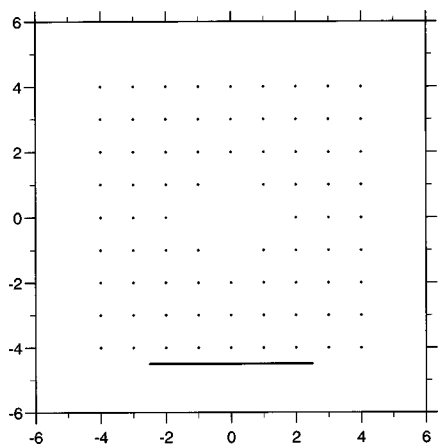

Fig. 13. 2D crystal with 9×9 wires ($d = 1$, $r = 0.01$). Here five central wires have been removed. The line below the crystal is the one used for the computation of the transmission factor.

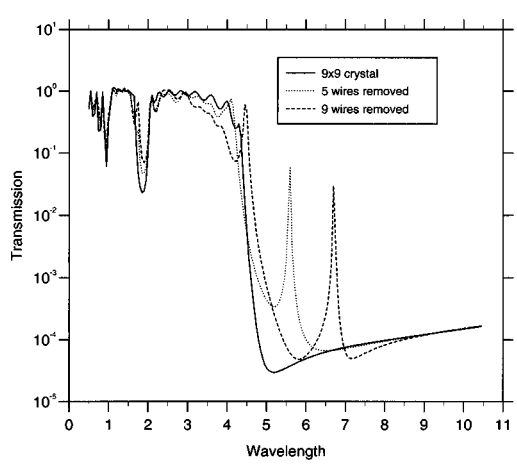

Fig. 14. Transmission factor versus wavelength for the crystal of Fig. 13. Solid curve, no defect; dotted and dashed curves, central wires removed as shown.

A. Influence of Defects on the Transmission

Starting from a crystal with $9 \times 9 = 81$ wires, we progressively remove some central wires. Figure 13 shows the positions of the wires when five wires have been removed at the center of the crystal. The radius of the wires is $r = d/100$. The transmission factor is computed in the following way: The crystal is illuminated in normal incidence by a plane wave coming from the top of Fig. 13. We compute the flux of the Poynting vector on a line lying below the crystal. The transmission factor is the ratio of this flux to the flux of the incident plane wave on the same line.

Figure 14 shows the transmission factor for a crystal with no defect and also when five and then nine central wires have been removed. For the crystal with no defect, the transmission factor behaves just as in Fig. 2: The light does not propagate inside the crystal for wavelengths greater than a cutoff wavelength λ_c. Another small gap, already observed in Fig. 2, appears at wavelengths close to 1.9. For large wavelengths the transmission increases a little, in contrast with the grating case. The reason comes from the fact that the line used for the computation of the transmission factor collects some energy flowing around the crystal, and this energy increases with the wavelength. By removing wires, one gets a cavity inside the crystal. The peaks observed in the transmission for $\lambda > \lambda_c$ are related to resonant modes of this cavity lying inside the (almost) opaque crystal. For $\lambda > \lambda_c$, the smaller cavity has only one mode, for $\lambda = 5.6$; whereas the larger cavity has two modes, for $\lambda = 6.7$ (fundamental mode) and for $\lambda = 4.45$. The field maps of these two modes are shown in Fig. 15. A more detailed study of the modes can be done by searching the complex resonant wavelengths associated with each of them.[9] The peaks observed in the transmission curves are due to the resonant cavity, which behaves as a relay for the photons, enabling them to cross the structure.

B. Mean-Field Theory

It was shown in Subsection 3.B that the metallic crystal behaves as a homogeneous material with real permittivity. Here we go a little bit further, and we highlight this property in the nonperiodic case.

In a first step, let us determine the homogenized permittivity of the crystal. We take a crystal made of 37 wires with radius $r = d/100$. All the wires lie in a circle with radius 3.2, and their positions are shown in Fig. 16. For a given wavelength we compute the diffracted field $E_{37}^d(\theta)$ upon a circle $\mathscr{C}$ containing all the wires (θ is the diffraction angle, and in the numerical process we took a circle of radius 10). Then, with the help of an iterative minimization technique, we get the characteristics (radius R, real permittivity ϵ) of a single homogeneous circular rod centered at the origin and giving the same diffracted field as the original set of 37 wires. More precisely, denoting by $E_1^d(\theta, R, \epsilon)$ the field diffracted by this homogeneous rod on $\mathscr{C}$, we minimize integral $\int_0^{2\pi} |E_{37}^d(\theta) - E_1^d(\theta, R, \epsilon)|^2 \mathrm{d}\theta$. We take an initial guess for R equal to 3.2, and the initial guess for ϵ is obtained from the theoretical limit value given by Eqs. (1) and (2).

Figure 17 shows the result of this homogenization process. The curve differs slightly from those of Fig. 5 ob-

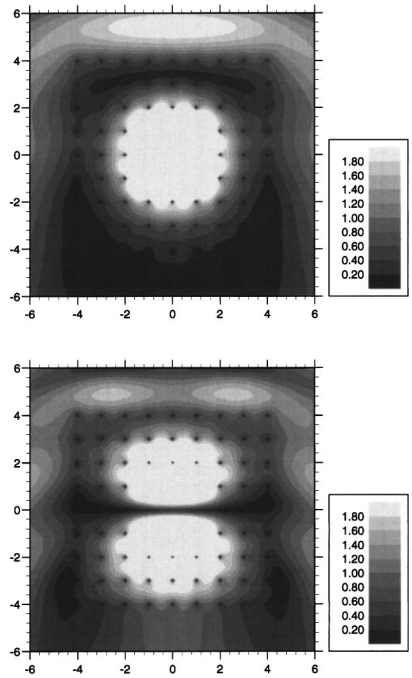

Fig. 15. Maps of the modulus of the total field for the crystal of Fig. 13 (nine central wires have been removed) illuminated with a plane wave at $\lambda = 6.7$ (upper map) and $\lambda = 4.45$ (lower map).

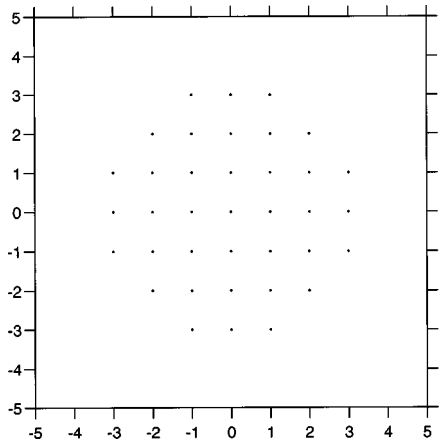

Fig. 16. Positions of the 37 wires used to illustrate the homogenization of a 2D finite crystal. The crystal is illuminated by a plane wave coming from the top. Wire spacing, $d = 1$; wire radius, $r = 10^{-2}$.

tained with the same crystal parameters (but in a periodic case). Nevertheless, the conclusion remains the same: Eqs. (1) and (2) obtained in the limit case of large wavelengths still give a good description of the behavior of the permittivity of the metallic crystal for short wavelengths. Consequently, for short wavelengths the crystal is equivalent to a homogeneous material with a positive permittivity (i.e., real optical index, possibly less than unity), and for large wavelengths it behaves as a material with negative permittivity (i.e., pure imaginary optical index). In the latter case the field vanishes rapidly in the material, which therefore becomes opaque.

Concerning the radius R, in the range of wavelengths going from 2 to 20, R always lies in the range 3.4–3.63. This means that, as in the periodic case (Subsection 3.B), the size of the homogenized material is slightly larger than the actual size of the crystal. Figures 18 and 19 compare the field maps obtained for two different wavelengths with the set of 37 wires and with the homogenized rod. Figure 18 is drawn for $\lambda = 4$. In this case the homogenized rod has a permittivity $\epsilon = 0.250$ (real optical index, 0.50) and a radius $R = 3.42$. Even if this wavelength is not large compared with the wire spacing, the two maps appear quite similar. This property is all the more surprising because the field must vanish on each wire in the nonhomogenized case (because of the boundary condition in this polarization case). Figure 19 is drawn for $\lambda = 10$. In this case the homogenized rod has

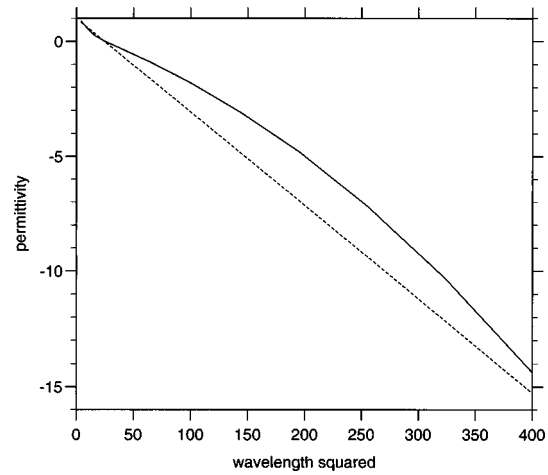

Fig. 17. Permittivity ϵ of a homogeneous rod equivalent to the 37 wires of Fig. 16. Solid curve, numerical result; dashed curve, the theoretical permittivity given by Eqs. (1) and (2).

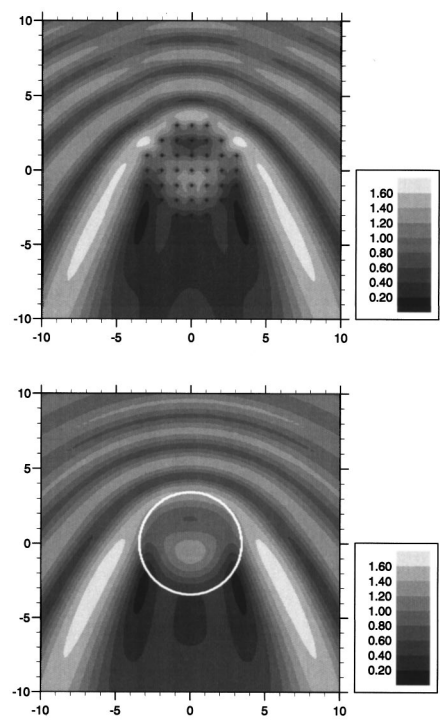

Fig. 18. Maps of the modulus of the total field for the set of 37 wires (upper map) and the homogenized rod (lower map) illuminated by a plane wave with $\lambda = 4$ coming from the top. White circle, actual dimension of the homogenized rod.

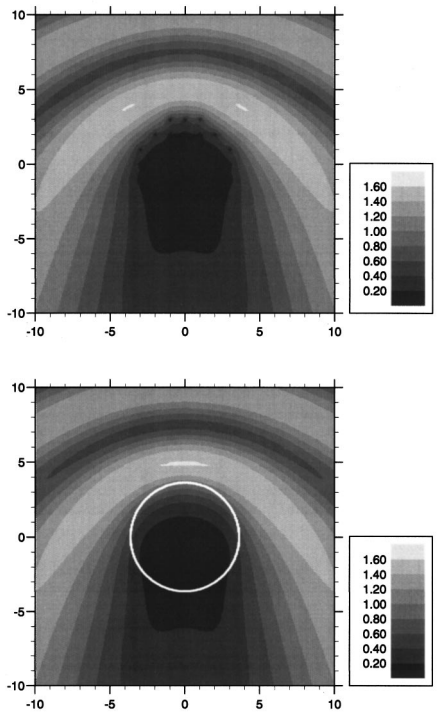

Fig. 19. Same as Fig. 18 but for $\lambda = 10$.

a permittivity $\epsilon = -1.81$ (imaginary optical index, $1.35i$) and a radius $R = 3.63$. Clearly, the set of wires is quite well represented by a homogeneous rod for this higher wavelength, and here the two maps are almost identical.

5. CONCLUSION

Two computer codes based on a rigorous theory of scattering have allowed us to investigate the gap properties of 2D metallic photonic crystals. It was found that the forbidden gaps of such structures extend from the null frequency to a cutoff value that depends on the crystal parameters. We also showed that a doped metallic crystal can have transmission peaks inside the gap.

However, the most important result deduced from our numerical results is that a 2D metallic photonic crystal can simulate a homogenized material, the plasmon frequency of which can be located in the microwave region. Moreover, it was shown that a good estimate of the permittivity at a given frequency can be given by a simple formula deduced from applied mathematics. Of course, the homogenization process considerably simplifies the problem of scattering by a metallic photonic crystal, and this simplification will be especially important for three-dimensional structures because of the numerical difficulty encountered in the modeling. We intend to present our first results in that field in a subsequent paper.

ACKNOWLEDGMENTS

The research described in this paper has been performed in the course of a contract between the Laboratoire d'Optique Électromagnétique and the Direction des Recherches, Études et Techniques (French Ministry of Defense).

REFERENCES

1. E. Yablonovitch, "Inhibited spontaneous emission in solid-state physics and electronics," Phys. Rev. Lett. **58**, 2059–2062 (1987).
2. S. John, "Strong localization of photons in certain disordered dielectric superlattices," Phys. Rev. Lett. **58**, 2486–2489 (1987).
3. J. Joannopoulos, R. Meade, and J. Winn, *Photonic Crystals* (Princeton U. Press, Princeton, N.J., 1995).
4. J. Rarity and C. Weisbuch, eds., *Microcavities and Photonic Bandgaps: Physics and Applications*, Vol. 324 of NATO Advanced Study Institute Series E (Kluwer, Dordrecht, The Netherlands, 1996).
5. D. Maystre, "Electromagnetic study of photonic band gaps," Pure Appl. Opt. **3**, 975–993 (1994).
6. C. Soukoulis, *Photonic Band Gaps and Localization* (Plenum, New York, 1993).
7. G. Kurizki and J. W. Haus, eds., special issue on photonic band structures, J. Mod. Opt. **41**, 173–404 (1994).
8. P. R. Bunker and T. J. Sears, feature on development and applications of materials exhibiting photonic band gaps, J. Opt. Soc. Am. B **10**, 171–413 (1993).
9. G. Tayeb and D. Maystre, "Rigorous theoretical study of finite size two-dimensional photonic crystals doped by microcavities," J. Opt. Soc. Am. A **14**, 3323–3332 (1997).
10. E. Ozbay, B. Temelkuran, M. Sigalas, G. Tuttle, C. Soukoulis, and K. Ho, "Defect structures in metallic photonic crystals," Appl. Phys. Lett. **69**, 3797–3799 (1996).
11. S. Cheng, R. Biswas, E. Ozbay, J. McCalmont, G. Tuttle, and K. Ho, "Optimized dipole antennas on photonic band gap crystal," Appl. Phys. Lett. **67**, 3399–3401 (1995).
12. E. Brown and O. McMahon, "High zenithal directivity from a dipole antenna on a photonic crystal," Appl. Phys. Lett. **68**, 1300–1302 (1996).
13. C. Maggiore, A. Clogston, G. Spalek, W. Sailor, and F. Mueller, "Low-loss microwave cavity using layered-dielectric materials," Appl. Phys. Lett. **64**, 1451–1453 (1994).
14. D. Smith, S. Schultz, N. Kroll, M. Sigalas, K. Ho, and C. Soukoulis, "Experimental and theoretical results for a two-dimensional metal photonic band-gap cavity," Appl. Phys. Lett. **65**, 645–647 (1994).
15. E. Brown and O. McMahon, "Large electromagnetic stop bands in metallodielectric photonic crystal," Appl. Phys. Lett. **67**, 2138–2140 (1995).
16. D. Felbacq, G. Tayeb, and D. Maystre, "Scattering by a random set of parallel cylinders," J. Opt. Soc. Am. A **11**, 2526–2538 (1994).
17. J. B. Pendry, "Calculating photonic band structure," J. Phys. Condens. Matter **8**, 1085–1108 (1996).
18. D. Felbacq, "Etude théorique et numérique de la diffraction de la lumierè par des ensembles de tiges parallèles," Ph.D. dissertation (Faculté St Jérôme, Marseille, France, 1994).
19. D. Felbacq and G. Bouchitté, "Homogenization of a set of parallel fibers," Waves Random Media **7**, 245–256 (1997).
20. D. Maystre and R. Petit, "Brewster incidence for metallic gratings," Opt. Commun. **17**, 196–200 (1976).
21. M. Hutley and D. Maystre, "The total absorption of light by a diffraction grating," Opt. Commun. **19**, 431–436 (1976).
22. J. B. Pendry, A. J. Holden, W. J. Stewart, and I. Youngs, "Extremely low frequency plasmons in metallic mesostructures," Phys. Rev. Lett. **76**, 4773–4776 (1996).